Azimuth-only Localization and Accuracy Study for Piecewise Curvilinearly Moving Targets

Marc Oispuu and **Julian Hörst**
Fraunhofer FKIE, Dept. Sensor Data and Information Fusion
Neuenahrer Str. 20, 53343 Wachtberg, Germany
{marc.oispuu, julian.hoerst}@fkie.fraunhofer.de

Abstract – *Passive tracking of maneuvering emitters is of fundamental interest. For this purpose, an appropriate motion model, the piecewise curvilinear motion model, is presented in this paper. The high-dimensional target state is characterized by position, speed, course, piecewise constant tangential and normal velocity, as well as maneuver change-over times. A single moving sensor collects azimuth measurements to obtain the target state. In order to determine the maximum achievable estimation accuracy, we derive the Cramér-Rao bounds for this estimation problem. A maximum likelihood estimator is propsed to solve the localization problem and to calculate the maneuver change-over times. Estimation results are obtained in Monte Carlo simulations and the efficiency of the estimator is proven by comparing these results with the theoretical Cramér-Rao bound.*

Keywords: Maneuvering targets, passive emitter localization, bearings-only tracking, Cramér-Rao bound, maximum likelihood estimation

1 Introduction

The estimation of the state (e.g. position, velocity) of an emitting source from passive bearing measurements collected by a single moving observer is a widely investigated problem. This problem is commonly referred to as Target Motion Analysis (TMA) [1] and is encountered in various fields like wireless communications, as well as airborne radar and underwater sonar applications. Aspects of the 2D and 3D TMA problem examined in the literature include bearings-only estimation algorithms, estimation accuracy, and target observability [1, 2].

In many cases, the targets are not moving inertially (i.e. non-accelerated), but are partly strongly maneuvering. Commonly maneuvering targets can be characterized by the curvilinear motion model described in [3] assuming constant and simultaneously active tangential (i.e. along-track) and normal (i.e. cross-track) acceleration a_t and a_n. An approximate solution of the curvilinear motion equation has also been presented in [3] for the case that the relative change of velocity is much lower than 1. The evaluation of the Cramér-Rao bound (CRB) has been realized in [4, 5] with the limited condition that the maneuver change-over times and the maneuvers are exactly known.

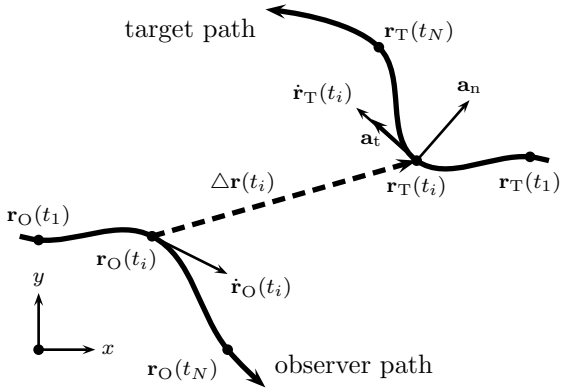

Figure 1: Geometry for the scenario of an arbitrary moving sensor and a piecewise curvilinearly moving target.

Only few papers have been published about solving the bearings-only tracking problem for maneuvering targets. E.g., a tracker using the interactive multiple model (IMM) approach has been proposed by Kirubarajan et al. [6]. In [7], a hidden Markov model (HMM) based tracking filter is presented. Moreover, an unscented Kalman filter (UKF) and a particle filter have been applied in [5]. However, all these approaches assume that the maneuver change-over times are not part of the estimation problem.

In this paper, we consider maneuvering targets performing a curvilinear motion in each maneuver segment (see Fig. 1) known as the *piecewise curvilinear motion* model established by Becker [8]. For this purpose, we present an exact solution of the motion equation which is necessary in order to evaluate the maximum achiev-

able estimation accuracy. Based on this solution, we derive the CRB for the estimation problem where maneuver change-over times are unknown, i.e. these parameters have to be estimated. In order to solve the TMA problem by means of azimuth measurements, we propose a maximum likelihood estimator (MLE).

This paper is organized as follows: In Section 2, we review Becker's target motion model for piecewise curvilinearly moving targets and formulate the problem. Subsequently, in Section 3, we derive the corresponding CRB, whereas in Section 4, we describe our TMA approach. The results demonstrating the performance of the MLE are presented in Section 5, and finally, conclusions and prospected future work are given in Section 6.

The following notations are used: $\mathbf{I}_n$ and $\mathbf{0}_n$ denote the $n \times n$-dimensional identity and zero matrix, $(\cdot)^T$ denotes transpose, and $\mathrm{E}\{\cdot\}$ denotes the expectation operation.

2 Estimation problem

We consider the scenario depicted in Fig. 1. A maneuvering target moves along a trajectory $\mathbf{r}_\mathrm{T}(t) = (x(t), y(t))^T$ with constant tangential acceleration $a_\mathrm{t} = |\mathbf{a}_\mathrm{t}|$ and normal acceleration $a_\mathrm{n} = |\mathbf{a}_\mathrm{n}|$. Furthermore, a single observer moves along an arbitrary trajectory $\mathbf{r}_\mathrm{O}(t) \in \mathbb{R}^{2\times 1}$. The target observer geometry is given by the relative vector

$$\triangle\mathbf{r}(t) = \begin{pmatrix}\triangle x(t)\\ \triangle y(t)\end{pmatrix} = \mathbf{r}_\mathrm{T}(t) - \mathbf{r}_\mathrm{O}(t)\,. \tag{1}$$

The observer's objective is to estimate the target state from passively measured line-of-sight azimuth angles α.

2.1 Curvilinear motion

The state of a target moving on a plane with constant tangential and normal acceleration can be completely described by the position components of $\mathbf{r}_\mathrm{T}(t)$, two velocity components given from the vector

$$\dot{\mathbf{r}}_\mathrm{T}(t) = \begin{pmatrix}\dot{x}(t)\\ \dot{y}(t)\end{pmatrix} = v(t)\begin{pmatrix}\sin\varphi(t)\\ \cos\varphi(t)\end{pmatrix}, \tag{2}$$

and the acceleration components a_t and a_n. The special cases of inertial motion ($a_\mathrm{t} = a_\mathrm{n} = 0$), straight-line acceleration ($a_\mathrm{t} \neq 0$, $a_\mathrm{n} = 0$), and circular motion ($a_\mathrm{t} = 0$, $a_\mathrm{n} \neq 0$) are included in this model. All target parameters are comprised in the parameter vector

$$\mathbf{x}(t) = \left(\mathbf{y}^T(t), a_\mathrm{t}, a_\mathrm{n}\right)^T \tag{3}$$

where $\mathbf{y}(t) = (x(t), y(t), v(t), \varphi(t))^T \in \mathbb{R}^{4\times 1}$. With this, a mathematical model of the target can be specified by the non-linear differential equation

$$\dot{\mathbf{x}}(t) = \begin{pmatrix} 0 & 0 & \sin\varphi(t) & 0 & 0 & 0\\ 0 & 0 & \cos\varphi(t) & 0 & 0 & 0\\ 0 & 0 & 0 & 0 & 1 & 0\\ 0 & 0 & 0 & 0 & 0 & v^{-1}(t)\\ 0 & 0 & 0 & 0 & 0 & 0\\ 0 & 0 & 0 & 0 & 0 & 0 \end{pmatrix}\mathbf{x}(t)\,. \tag{4}$$

An approximate solution of the aforementioned motion equation, $\mathbf{x}(t) = \mathbf{\Phi}(t, t_0)\,\mathbf{x}(t_0)$, can be found in [3]. We obtain the exact solution of the initial value problem (4) by

$$\mathbf{x}(t) = \mathbf{f}[\mathbf{x}(t_0); t, t_0] \tag{5}$$

which describes the temporally evolution of the target state from t_0 to t. The components of (5) are given in Appendix A.1. Mentionable, the initial time t_0 can be replaced by any reference time $t_\mathrm{r} > t_0$. The state at t_r can be written shortly as $\mathbf{x}_\mathrm{r} = \mathbf{x}(t_\mathrm{r})$.

2.2 Piecewise curvilinear motion

In the case of piecewise curvilinear motion, the dimension of the state vector in (3) increases by three components with each maneuver change-over. That means, two acceleration components and the maneuver change-over time are added to the state vector. With M maneuvers, the augmented state vector is specified by

$$\mathbf{x}(t) = \left(\mathbf{y}^T(t), \mathbf{a}^T, \tilde{\mathbf{t}}^T\right)^T \tag{6}$$

with $\mathbf{a} = (a_{\mathrm{t},0}, a_{\mathrm{n},0}, ..., a_{\mathrm{t},M}, a_{\mathrm{n},M})^T \in \mathbb{R}^{2(M+1)\times 1}$ and $\tilde{\mathbf{t}} = (\tilde{t}_1, ..., \tilde{t}_M)^T \in \mathbb{R}^{M\times 1}$. Here, $\tilde{t}_m$ is the change-over time of the m-th maneuver and $a_{\mathrm{t},m}$ and $a_{\mathrm{n},m}$ denote the tangential and normal acceleration in the time interval $[\tilde{t}_{m-1}, \tilde{t}_m]$, $m = 1, ..., M$.

Similar to Section 2.1, the target state can be parameterized by the state at another time, e.g. by $\mathbf{x}_m = \mathbf{x}(\tilde{t}_m)$. Since the reference state is commonly the current target state, the target state for M maneuvers in the time interval $[t_0, t_\mathrm{r}]$ is given by

$$\mathbf{x}(t) = \begin{cases} \mathbf{f}[\mathbf{x}_1; t, \tilde{t}_1] & \text{for } t_0 \le t \le \tilde{t}_1\\ \vdots & \vdots\\ \mathbf{f}[\mathbf{x}_m; t, \tilde{t}_m] & \text{for } \tilde{t}_{m-1} < t \le \tilde{t}_m\\ \vdots & \vdots\\ \mathbf{f}[\mathbf{x}_M; t, \tilde{t}_M] & \text{for } \tilde{t}_{M-1} < t \le \tilde{t}_M\\ \mathbf{f}[\mathbf{x}_\mathrm{r}; t, t_\mathrm{r}] & \text{for } \tilde{t}_M < t \le t_\mathrm{r} \end{cases}, \tag{7}$$

where the target state at some arbitrary time t is related to the reference state by

$$\mathbf{f}[\mathbf{x}_m; t, \tilde{t}_m] = \mathbf{f}[\mathbf{f}[\cdots\mathbf{f}[\mathbf{x}_\mathrm{r}; t, t_\mathrm{r}]; \cdots]; t, \tilde{t}_m]\,. \tag{8}$$

2.3 Measurement model

For the sake of simplicity, we assume that the detection probability is equal to 1 and the false alarm rate is equal to 0. The measured azimuth α_m at time t_i, $i = 1, ..., N$, is given by

$$\alpha_\mathrm{m}(t_i) = \alpha(t_i) + w_\alpha(t_i)\,, \tag{9}$$

where $w_\alpha(t_i)$ denotes the measurement error and

$$\alpha(t) = \arctan\frac{\triangle x(t)}{\triangle y(t)} \tag{10}$$

is the true azimuth angle. The observer position $\mathbf{r}_\mathrm{O}(t)$ is assumed to be exactly known. With this, (10) only depends on the target state. The components $\alpha_\mathrm{m}(t_i)$, $\alpha(t_i)$, and $w_\alpha(t_i)$ can be written in compact vector form

$$\boldsymbol{\alpha}_\mathrm{m} = \boldsymbol{\alpha} + \mathbf{w}_\alpha\,, \tag{11}$$

where $\mathbf{w}_\alpha$ denotes the N-dimensional noise vector with the covariance matrix $\mathbf{W}_\alpha$. We assume that the measurement noise is zero-mean Gaussian and the measurement covariance reads $\mathbf{W}_\alpha = \sigma_\alpha^2\,\mathbf{I}_N$, where σ_α^2 denotes the constant noise variance. We note that in practice, the variances may change from time to time and have to be estimated.

With the previous considerations, the problem can be stated as follows: Estimate the target state $\mathbf{x}_\mathrm{r}$ at some reference time t_r from all measurements $\boldsymbol{\alpha}_\mathrm{m}$.

3 Cramér-Rao bound (CRB)

The CRB provides a lower bound on the estimation accuracy and its parameter dependencies reveal characteristic features of the estimation problem. The target parameters are comprised in the vector $\mathbf{x}_\mathrm{r}$. In this case, the CRB is related to the covariance matrix $\mathbf{C}$ of the estimation error $\triangle\mathbf{x}_\mathrm{r} = \mathbf{x}_\mathrm{r} - \hat{\mathbf{x}}_\mathrm{r}(\boldsymbol{\alpha})$ of any unbiased estimator $\hat{\mathbf{x}}_\mathrm{r}(\boldsymbol{\alpha})$ as

$$\mathbf{C} = \mathrm{E}\left\{\triangle\mathbf{x}_\mathrm{r}\,\triangle\mathbf{x}_\mathrm{r}^T\right\} \geq \mathbf{J}^{-1}(\mathbf{x}_\mathrm{r})\,, \tag{12}$$

where the inequality means that the matrix difference is positive semidefinite. If the estimator attains the CRB then it is called *efficient*. The CRB is given by the inverse Fisher Information Matrix (FIM)

$$\mathbf{J}(\mathbf{x}_\mathrm{r}) = \mathrm{E}\left\{\left(\frac{\partial\mathcal{L}(\boldsymbol{\alpha};\mathbf{x}_\mathrm{r})}{\partial\mathbf{x}_\mathrm{r}}\right)^T\left(\frac{\partial\mathcal{L}(\boldsymbol{\alpha};\mathbf{x}_\mathrm{r})}{\partial\mathbf{x}_\mathrm{r}}\right)\right\}, \tag{13}$$

where

$$\mathcal{L} = -\frac{1}{2}\ln\left(\det(2\pi\mathbf{W}_\alpha)\right) - \frac{1}{2}(\boldsymbol{\alpha}_\mathrm{m} - \boldsymbol{\alpha})^T\,\mathbf{W}_\alpha^{-1}(\boldsymbol{\alpha}_\mathrm{m} - \boldsymbol{\alpha}) \tag{14}$$

is the log-likelihood function. In this log-likelihood function, $\boldsymbol{\alpha}$ are random variables due to the random variables $\mathbf{w}_\alpha$. Inserting (14) into (13), performing the expectation operation, and using the noise covariance in Section 2.3, we obtain the FIM

$$\mathbf{J}(\mathbf{x}_\mathrm{r}) = \frac{1}{\sigma_\alpha^2}\sum_{i=1}^{N}\left(\frac{\partial\alpha(t_i)}{\partial\mathbf{x}_\mathrm{r}}\right)^T\frac{\partial\alpha(t_i)}{\partial\mathbf{x}_\mathrm{r}} \tag{15}$$

for the azimuth-only case. It is important to emphasize that the above given FIMs denote the maximum achievable information at an arbitrary reference time t_r based on N measurements. The partial derivations in (15) are calculated by the chain rule:

$$\frac{\partial\alpha(t_i)}{\partial\mathbf{x}_\mathrm{r}} = \frac{\partial\mathbf{x}(t_i)}{\partial\mathbf{x}_\mathrm{r}}\frac{\partial\alpha(t_i)}{\partial\mathbf{x}(t_i)}\,. \tag{16}$$

The derivation of $\alpha(t_i)$ follows from (10):

$$\frac{\partial\alpha(t_i)}{\partial\mathbf{x}(t_i)} = \frac{1}{\triangle r^2(t_i)}\begin{pmatrix}\triangle y(t_i)\\ -\triangle x(t_i)\\ 0\\ \vdots\\ 0\end{pmatrix}^T \in \mathbb{R}^{1\times 6+3M}\,, \tag{17}$$

where $\triangle r(t) = |\triangle\mathbf{r}(t)|$ denotes the distance between observer and target (see also (1)).

For the special case of purely curvilinear motion, no maneuver change has to be regarded. Therefore, the derivation $\partial\mathbf{x}(t_i)/\partial\mathbf{x}_\mathrm{r}$ is simply the Jacobian matrix of the vector-valued function (5) at time $t = t_i$:

$$\frac{\partial\mathbf{x}(t_i)}{\partial\mathbf{x}_\mathrm{r}} = \left.\frac{\partial\mathbf{f}[\mathbf{x}(t_0);t,t_0]}{\partial\mathbf{x}_\mathrm{r}}\right|_{t=t_i}\,. \tag{18}$$

At this point we mention that the exact solution of the motion equation in (5) is necessary to evaluate the Jacobian matrix in (18). The components of (18) are given in Appendix A.2.

For the more general case of piecewise curvilinear motion with M maneuver changes, we have to express the Jacobian matrix $\partial\mathbf{x}(t_i)/\partial\mathbf{x}_\mathrm{r}$ w.r.t. several target maneuvers enclosed in the vector $\tilde{\mathbf{t}}$ as well as different tangential and normal accelerations represented by the vector $\mathbf{a}$ in (6).

Since we assume the reference time to be the current time, the relative displacement of t_i and t_r regarding the maneuvers make it necessary to distinguish between

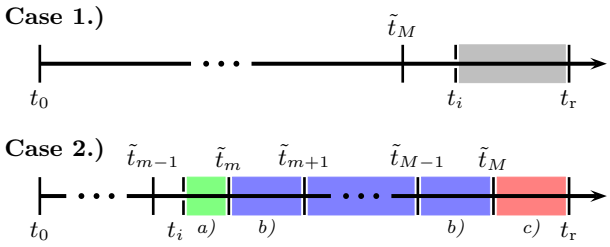

Figure 2: Relative displacement of time t_i and reference time t_r.

two different cases (Fig. 2): 1.) t_i and t_r lie in the same maneuver segment, and 2.) the segment containing t_i is occurred before the segment containing t_r.

Throughout the subsequent evaluations, we will need the derivations given by

$$\frac{\partial \mathbf{y}(t_i)}{\partial t} = \left(v(t)\sin\varphi(t), v(t)\cos\varphi(t), a_\mathrm{t}, \frac{a_\mathrm{n}}{v(t)} \right)^T ,$$
$$\frac{\partial \mathbf{y}(t_i)}{\partial t_\mathrm{r}} = -\frac{\partial \mathbf{y}(t_i)}{\partial t} . \tag{19}$$

Case 1.) $\tilde{t}_M \leq t_i \leq t_\mathrm{r}$: If the measurement time t_i and the reference time t_r are in the same maneuver segment, no maneuver changes have to be considered. Hence, the $6+3M \times 6+3M$ Jacobian matrix $\partial \mathbf{x}(t_i)/\partial \mathbf{x}_\mathrm{r}$ is given by

$$\frac{\partial \mathbf{x}(t_i)}{\partial \mathbf{x}_\mathrm{r}} = \begin{pmatrix} \frac{\partial \mathbf{y}(t_i)}{\partial \mathbf{y}_\mathrm{r}} & \frac{\partial \mathbf{y}(t_i)}{\partial \mathbf{a}} & \mathbf{0} \\ \mathbf{0} & \mathbf{I} & \mathbf{0} \\ \mathbf{0} & \mathbf{0} & \mathbf{I} \end{pmatrix} \tag{20}$$

with

$$\frac{\partial \mathbf{y}(t_i)}{\partial \mathbf{a}} = \left(\mathbf{0}, \frac{\partial \mathbf{y}(t_i)}{\partial a_{\mathrm{t},M}}, \frac{\partial \mathbf{y}(t_i)}{\partial a_{\mathrm{n},M}} \right) \in \mathbb{R}^{4\times 2(M+1)} .$$

The partial derivations $\partial \mathbf{y}(t_i)/\partial \mathbf{y}_\mathrm{r}$, $\partial \mathbf{y}(t_i)/\partial a_{\mathrm{t},M}$, and $\partial \mathbf{y}(t_i)/\partial a_{\mathrm{n},M}$ are specified in Appendix A.2. They are calculated by replacing t with t_i, a_t with $a_{\mathrm{t},M}$, and a_n with $a_{\mathrm{n},M}$ in the equations given there.

Case 2.) $\tilde{t}_{m-1} \leq t_i < \tilde{t}_m$, $m = 1, \ldots, M$: In this case, the target state consists of several nested single segment transitions (8) and therefore depends on $\tilde{\mathbf{t}}$. By applying the chain rule, the Jacobian matrix can be written as

$$\frac{\partial \mathbf{x}(t_i)}{\partial \mathbf{x}_\mathrm{r}} = \underbrace{\frac{\partial \mathbf{x}(t_i)}{\partial \mathbf{x}_m}}_{a)} \underbrace{\frac{\partial \mathbf{x}_m}{\partial \mathbf{x}_{m+1}} \cdots \frac{\partial \mathbf{x}_{M-1}}{\partial \mathbf{x}_M}}_{b)} \underbrace{\frac{\partial \mathbf{x}_M}{\partial \mathbf{x}_\mathrm{r}}}_{c)} . \tag{21}$$

It can be recognized that the above equation contains three qualitatively different classes of matrices whose solutions are derived in the following paragraphs *a)*, *b)*, and *c)*.

a) $\partial \mathbf{x}(t_i)/\partial \mathbf{x}_m$ is the Jacobian matrix describing the transition from t_i to the lower bound $\tilde{t}_m$ of the following maneuver segment having the following form:

$$\frac{\partial \mathbf{x}(t_i)}{\partial \mathbf{x}_m} = \begin{pmatrix} \frac{\partial \mathbf{y}(t_i)}{\partial \mathbf{y}_m} & \frac{\partial \mathbf{y}(t_i)}{\partial \mathbf{a}} & \frac{\partial \mathbf{y}(t_i)}{\partial \tilde{\mathbf{t}}} \\ \mathbf{0} & \mathbf{I} & \mathbf{0} \\ \mathbf{0} & \mathbf{0} & \mathbf{I} \end{pmatrix} \tag{22}$$

with

$$\frac{\partial \mathbf{y}(t_i)}{\partial \mathbf{a}} = \left(\mathbf{0}, \frac{\partial \mathbf{y}(t_i)}{\partial a_{\mathrm{t},m-1}}, \frac{\partial \mathbf{y}(t_i)}{\partial a_{\mathrm{n},m-1}}, \mathbf{0} \right) \in \mathbb{R}^{4\times 2(M+1)} ,$$
$$\frac{\partial \mathbf{y}(t_i)}{\partial \tilde{\mathbf{t}}} = \left(\mathbf{0}, \frac{\partial \mathbf{y}(t_i)}{\partial \tilde{t}_m}, \mathbf{0} \right) \in \mathbb{R}^{4\times M} .$$

See Appendix A.2 and (19) for the above partial derivations. In order to perform these derivations, one has to replace $\mathbf{y}_\mathrm{r}$ by $\mathbf{y}_m$, t_r by $\tilde{t}_m$, t by t_i, a_t by $a_{\mathrm{t},m-1}$, and a_n by $a_{\mathrm{n},m-1}$.

b) $\partial \mathbf{x}_m/\partial \mathbf{x}_{m+1}$ represents the class of Jacobian matrices which describes the transitions from the lower to the upper bound of a maneuver segment. It can be expressed by

$$\frac{\partial \mathbf{x}_m}{\partial \mathbf{x}_{m+1}} = \begin{pmatrix} \frac{\partial \mathbf{y}_m}{\partial \mathbf{y}_{m+1}} & \frac{\partial \mathbf{y}_m}{\partial \mathbf{a}} & \frac{\partial \mathbf{y}_m}{\partial \tilde{\mathbf{t}}} \\ \mathbf{0} & \mathbf{I} & \mathbf{0} \\ \mathbf{0} & \mathbf{0} & \mathbf{I} \end{pmatrix} \tag{23}$$

with

$$\frac{\partial \mathbf{y}_m}{\partial \mathbf{a}} = \left(\mathbf{0}, \frac{\partial \mathbf{y}_m}{\partial a_{\mathrm{t},m}}, \frac{\partial \mathbf{y}_m}{\partial a_{\mathrm{n},m}}, \mathbf{0} \right) \in \mathbb{R}^{4\times 2(M+1)} ,$$
$$\frac{\partial \mathbf{y}_m}{\partial \tilde{\mathbf{t}}} = \left(\mathbf{0}, \frac{\partial \mathbf{y}_m}{\partial \tilde{t}_m}, \frac{\partial \mathbf{y}_m}{\partial \tilde{t}_{m+1}}, \mathbf{0} \right) \in \mathbb{R}^{4\times M} .$$

Also here, Appendix A.2 and (19) contain the above partial derivations. The current replacement rules are: substitute $\mathbf{y}_\mathrm{r}$ by $\mathbf{y}_{m+1}$, t_r by $\tilde{t}_{m+1}$, t by $\tilde{t}_m$, a_t by $a_{\mathrm{t},m}$, and a_n by $a_{\mathrm{n},m}$.

c) Finally, $\partial \mathbf{x}_M/\partial \mathbf{x}_\mathrm{r}$ for the transition from the upper bound $\tilde{t}_M$ of maneuver segment M to the reference time t_r is given by

$$\frac{\partial \mathbf{x}_M}{\partial \mathbf{x}_\mathrm{r}} = \begin{pmatrix} \frac{\partial \mathbf{y}_M}{\partial \mathbf{y}_\mathrm{r}} & \frac{\partial \mathbf{y}_M}{\partial \mathbf{a}} & \frac{\partial \mathbf{y}_M}{\partial \tilde{\mathbf{t}}} \\ \mathbf{0} & \mathbf{I} & \mathbf{0} \\ \mathbf{0} & \mathbf{0} & \mathbf{I} \end{pmatrix} \tag{24}$$

with

$$\frac{\partial \mathbf{y}_M}{\partial \mathbf{a}} = \left(\mathbf{0}, \frac{\partial \mathbf{y}_M}{\partial a_{\mathrm{t},M}}, \frac{\partial \mathbf{y}_M}{\partial a_{\mathrm{n},M}} \right) \in \mathbb{R}^{4\times 2(M+1)} ,$$
$$\frac{\partial \mathbf{y}_M}{\partial \tilde{\mathbf{t}}} = \left(\mathbf{0}, \frac{\partial \mathbf{y}_M}{\partial \tilde{t}_M} \right) \in \mathbb{R}^{4\times M} .$$

When performing the above partial derivations using Appendix A.2 and (19), one has to substitute t by $\tilde{t}_M$, a_t by $a_{\mathrm{t},M}$, and a_n by $a_{\mathrm{n},M}$.

4 TMA approach

One of the most important methods to estimate a constant parameter set is the maximum likelihood estimator (MLE). For the TMA problem specified in Section 2, the MLE is given by the maximization of the log-likelihood function in (14). Thus, the MLE minimizes the quadratic form

$$f_\alpha(\mathbf{x}_\mathrm{r}) = \frac{1}{\sigma_\alpha^2} \sum_{i=1}^{N} \left| \alpha_\mathrm{m}(t_i) - \alpha(\mathbf{x}(t_i)) \right|^2 \tag{25}$$

for the azimuth-only case, where the target state $\mathbf{x}(t_i)$ is related to the reference state $\mathbf{x}_\mathrm{r} = \mathbf{x}(t_\mathrm{r})$ by (5) for curvilinearly moving targets or by (7) for piecewise curvilinearly moving targets. In this way, the unknown maneuver change-over times are part of the estimation problem. We estimate the complete parameter vector given

in (6) from the complete measurement set. Note, that the parameter increases by three components with each maneuver change. The cost function displays a global minimum for a proper choice of $\mathbf{x}_\mathrm{r}$.

For a piecewise curvilinear motion, the aforementioned cost function is parameterized by a $(6+3M)$-dimensional state vector including the unknown maneuver change-over times. The choice of the correct state vector dimension requires the knowledge of the maneuver changes M, but in practice, this number is unknown. Commonly, chi-square tests on, e.g., accelerations are used to detect the begin and the end of maneuvers. Alternatively, an estimation technique can be used based on a state vector including only a single maneuver change:

$$\mathbf{x}(t) = \left(\mathbf{y}^T(t), a_{\mathrm{t},m-1}, a_{\mathrm{n},m-1}, a_{\mathrm{t},m}, a_{\mathrm{n},m}, \tilde{t}_m\right)^T .$$

The m-th maneuver change is detected if the accuracy of the maneuver change-over time estimates is sufficiently precise and/or the acceleration estimates between the segments are sufficiently different. However, we assume that the number of maneuver changes M is known but the maneuver change-over times are unknown.

5 Simulation results

We consider the 2D scenario in Fig. 3. The target starts with the initial state $\mathbf{y}_0 = (0\,\mathrm{m}, 0\,\mathrm{m}, 50\,\mathrm{m/s}, 90°)^T$ and performs the following maneuvers:

$$\begin{aligned}(t_0, a_{\mathrm{t},0}, a_{\mathrm{n},0}) &= (0\,\mathrm{s}, 0\,\mathrm{m/s^2}, 0\,\mathrm{m/s^2})\,,\\ (\tilde{t}_1, a_{\mathrm{t},1}, a_{\mathrm{n},1}) &= (200\,\mathrm{s}, 0\,\mathrm{m/s^2}, 1.047\,\mathrm{m/s^2})\,,\\ (\tilde{t}_2, a_{\mathrm{t},2}, a_{\mathrm{n},2}) &= (400\,\mathrm{s}, 0.2\,\mathrm{m/s^2}, 0\,\mathrm{m/s^2})\,.\end{aligned}$$

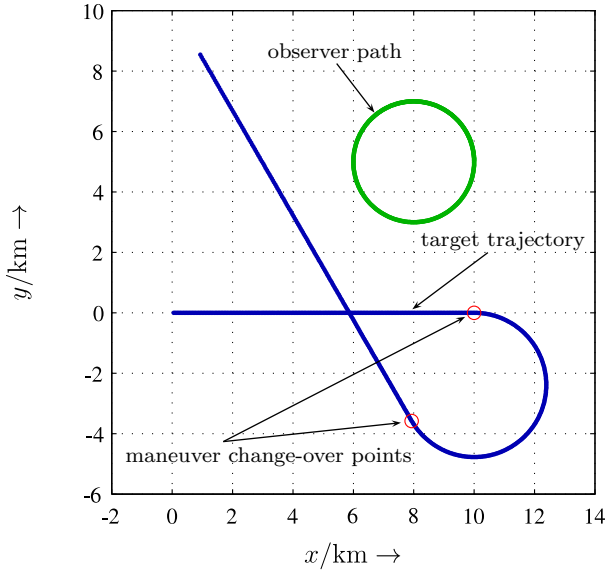

Figure 3: Observer path and target trajectory with maneuver change-over points.

The observer moves counterclockwise along a circular path with a constant velocity. This is parameterized by $\mathbf{r}_\mathrm{O}(t_0) = (10\,\mathrm{km}, 5\,\mathrm{km})^T$, $|\dot{\mathbf{r}}_\mathrm{O}(t_0)| = 50\,\mathrm{m/s}$, $\varphi_\mathrm{O}(t_0) = 0°$, and $a_{\mathrm{O,n}} = -1.25\,\mathrm{m/s^2}$. From the observability condition established in [2], it follows that the state of an inertial moving target can be determined from azimuth measurements obtained from a sensor moving on a circular path, i.e., for the considered scenario the uniqueness condition is already fulfilled in the first segment of the target trajectory.

The sensor collects one measurement each second, i.e., 200 measurements per maneuver segment. The measurement noise vectors are zero-mean Gaussian with the covariances given in Section 2.3 and the corresponding standard deviations $\sigma_\alpha = 3°$.

5.1 Cramér-Rao analysis

For the Cramér-Rao analysis, we use Cartesian velocity components instead of the given polar velocity components because these are more insightful for illustrating the CRBs. The FIM in (15) can be easily transformed in Cartesian coordinates by using a suitable transformation.

In Fig. 4, the CRBs for the considered scenario are depicted. The subfigures show the individual bounds w.r.t. the state vector with a maximum of 12 components, namely (in correct order) for the position x, y, for the Cartesian velocity $\dot{x}$, $\dot{y}$, for the tangential and normal accelerations $a_{\mathrm{t},0}$, $a_{\mathrm{t},1}$, $a_{\mathrm{t},2}$, and $a_{\mathrm{n},0}$, $a_{\mathrm{n},1}$, $a_{\mathrm{n},2}$, as well as for the two maneuver change-over times $\tilde{t}_1$, $\tilde{t}_2$ regarding the three maneuver segments. Note, that when a maneuver change takes place at time $\tilde{t}_m \in \{400\,\mathrm{s}, 600\,\mathrm{s}\}$ (depicted by the dashed vertical lines), the dimension of the state vector increases by three elements: $a_{\mathrm{t},m}$, $a_{\mathrm{n},m}$, and $\tilde{t}_m$ are added. So, the state vector consists of six elements for t_0 and of 12 elements for $t_\mathrm{max} = 600\,\mathrm{s}$.

It can be recognized that the estimation accuracy increases with a growing number of measurements. This is clear since the Fisher information is added up over all previous measurements (see also (15)). At maneuver changes, the dimension of the FIM and therefore of the entire estimation problem increases since the state vector has three new elements. Hence, the estimation accuracy decreases. A further reason for this are the acceleration components: They have rapidly altered since the last maneuver change-over and are effectual for a short time, so that only a few measurements can support them.

5.2 Accuracy study

For the considered scenario, Monte Carlo simulations with 1000 runs have been carried out to study the performance of the estimator given in Section 4. In our simulations, we use the simplex method of Nelder and Mead [9] to find the minima of the cost function (25) and we initialize every search with the true value. For

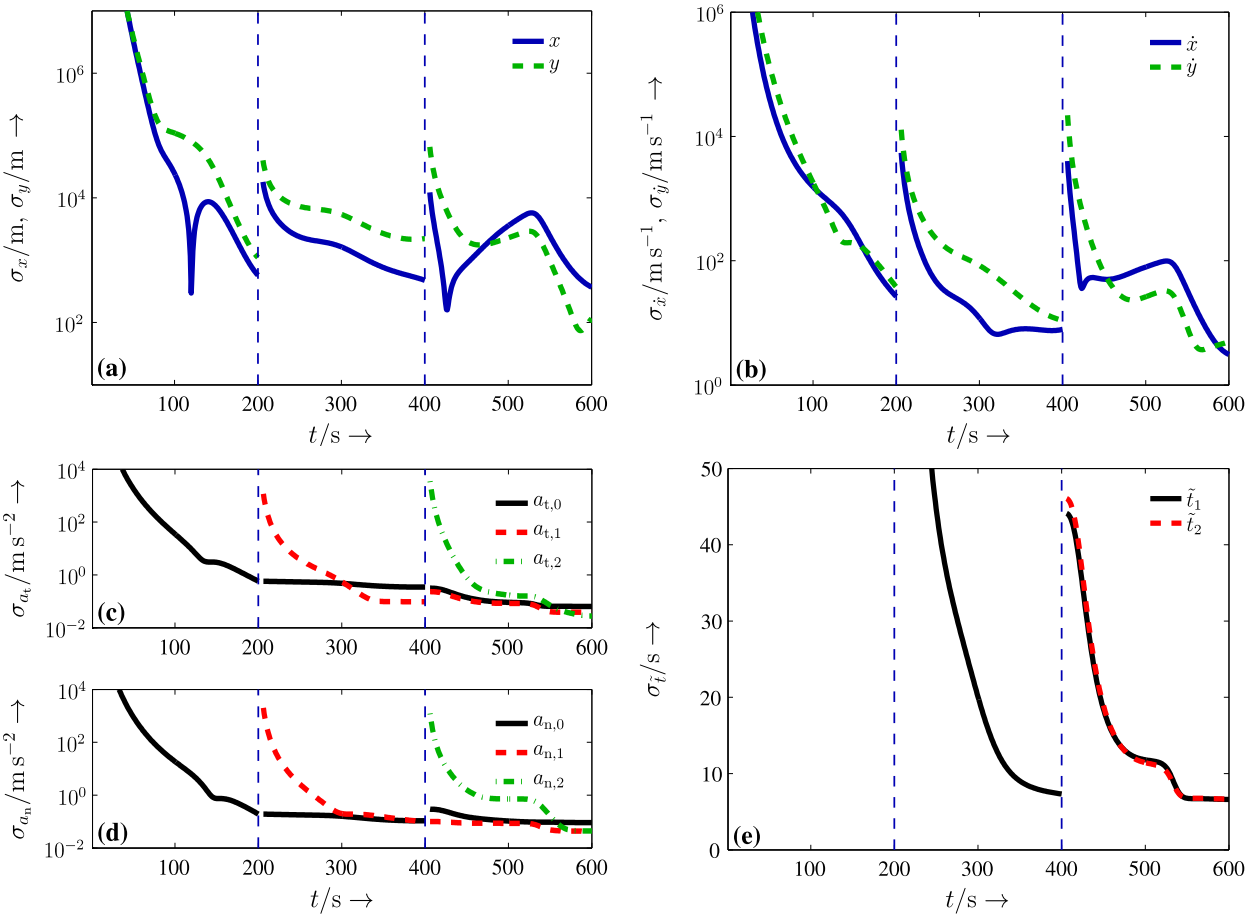

Figure 4: CRBs for the considered scenario: (a) position x and y; (b) Cartesian velocity $\dot{x}$ and $\dot{y}$; (c) tangential accelerations $a_{\mathrm{t},0}$, $a_{\mathrm{t},1}$, $a_{\mathrm{t},2}$ for the three maneuver segments; (d) normal accelerations $a_{\mathrm{n},0}$, $a_{\mathrm{n},1}$, $a_{\mathrm{n},2}$; and (e) maneuver change-over times $\tilde{t}_1$, $\tilde{t}_2$.

the sake of simplicity, we use also the Cartesian velocity components to solve the optimization problem.

Firstly, we consider the case of $N = 600$ measurements. Therefore, the target performs two maneuvers and the state vector contains 12 parameters. Fig. 5 shows the xy-plane of the cost function with fixed remaining parameters. The cost function displays a well-pronounced minimum near by the true target location and no further local minima. We find similar results for other cuts trough the cost function.

The scattering of the Monte Carlo estimates around the true values can be visualized, e.g., through scatter plots of the estimation error. Mathematically, the scattering of the projected sample values is adequately described by the projection of the estimation error covariance in (12) onto the respective 2D subspaces. The resulting 2D estimation error ellipses are compared with the corresponding (Cramér-Rao) bound ellipses (Fig. 6). The ellipse parameters were chosen in such a way that, assuming normally distributed estimation errors, the ellipses enclose 95.4% (2σ-ellipse) of the sample values.

Fig. 6 shows estimation error ellipses for $N = 400$.

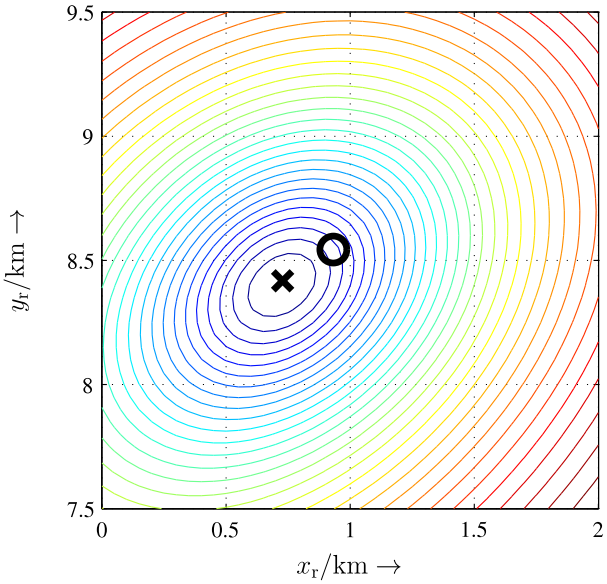

Figure 5: Cut through cost function with true (circle) and estimated (cross) target location.

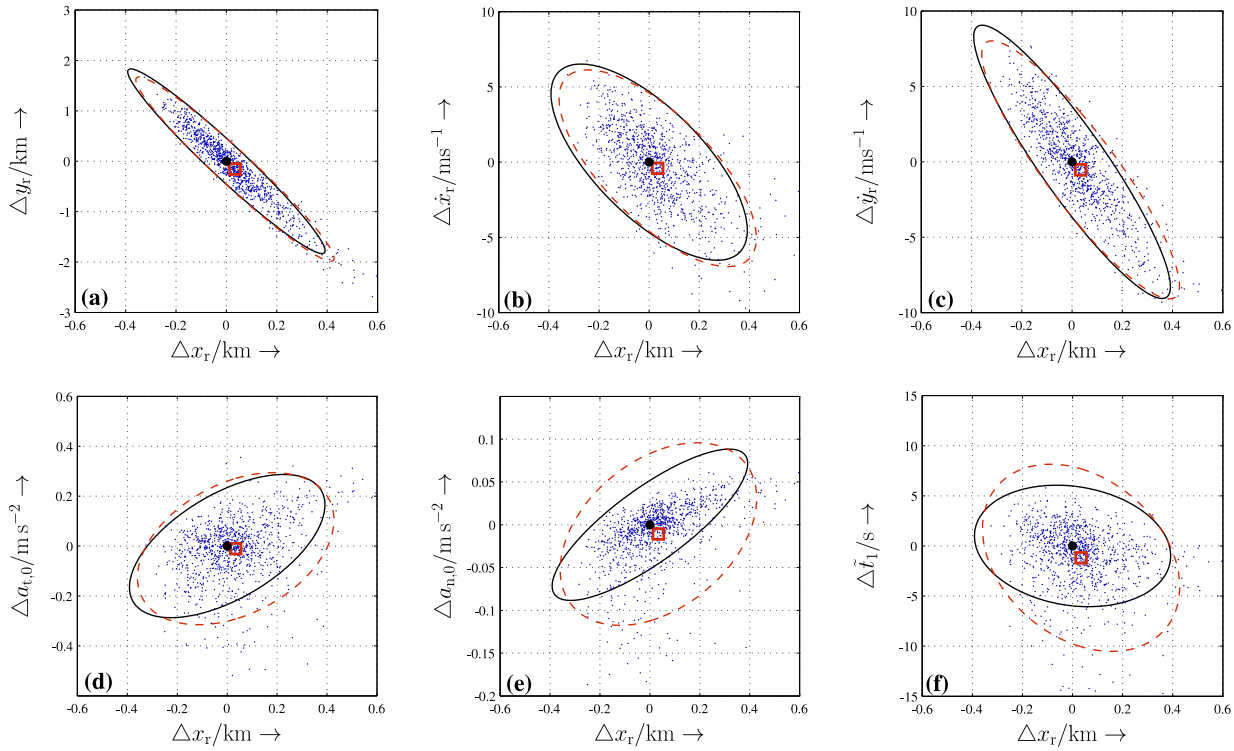

Figure 6: Scatter plots of the estimation error (blue dots) with estimation error mean (red quad), estimation error ellipse (red dashed line), and Cramér-Rao bound ellipse (black solid line).

The estimation error ellipses and bound ellipses have a similar orientation and expansion. The scatter plots display that the estimation results are biased, but it is well-known that the MLE is asymptotically efficient, i.e., the estimates are biased in the presence of noise and for a finite number of measurements N. Overall, we find a good consistency between the estimation ellipses and bound ellipses, especially for the estimates of $\mathbf{y}_\mathrm{r}$. Furthermore, the scatter plots prove that the target maneuvering time can be estimated, even if the error ellipse deviates from the bound ellipse in this case.

6 Conclusions

The considered target motion model subsumes the models described in the literature. We have presented an exact solution of the corresponding motion equation and have derived the CRB for the case that the maneuver accelerations and change-over times are unknown. In a Cramér-Rao analysis, we have found that the extension of the target state by acceleration components and change-over times leads to a declined estimation accuracy. Nevertheless, we have proposed an MLE which is able to estimate the target state parameters including the unknown maneuver change-over times. In Monte Carlo simulations, we have proven that the achieved estimation accuracy corresponds to the expected accuracy given by the CRB. Future work may also exploit additional measurements, e.g. the azimuth rate $\dot{\alpha}$, and may include the development of a recursive filter.

A Derivations

The following substitutions are used in this appendix:

$$
\begin{aligned}
c_\mathrm{a} &= (4a_\mathrm{t}^2 + a_\mathrm{n}^2)^{-1}\,, \\
S(t) &= (2a_\mathrm{t}\sin\varphi(t) - a_\mathrm{n}\cos\varphi(t))v^2(t)\,, \\
T(t) &= (2a_\mathrm{t}\cos\varphi(t) + a_\mathrm{n}\sin\varphi(t))v^2(t)\,, \\
\triangle t &= t - t_\mathrm{r}\,, \\
\triangle S &= S(t) - S(t_\mathrm{r})\,, \\
\triangle T &= T(t) - T(t_\mathrm{r})\,.
\end{aligned}
$$

A.1 Components of $\mathbf{f}[\mathbf{x}_\mathrm{r}; t, t_\mathrm{r}]$

The solution by initial value problem are given by (5). The components of $\mathbf{f}[\mathbf{x}_\mathrm{r}; t, t_\mathrm{r}]$ depending on the initial value $\mathbf{x}_\mathrm{r} = (x_\mathrm{r}, y_\mathrm{r}, v_\mathrm{r}, \varphi_\mathrm{r}, a_\mathrm{t}, a_\mathrm{n})^T$ are specified by

$$
x(t) = \begin{cases} x_\mathrm{r} + c_\mathrm{a}\,\triangle S & \text{for } a_\mathrm{t} \vee a_\mathrm{n} \neq 0 \\ x_\mathrm{r} + \triangle t\, v_\mathrm{r}\sin\varphi_\mathrm{r} & \text{for } a_\mathrm{t} \wedge a_\mathrm{n} = 0 \end{cases}, \tag{26}
$$

$$
y(t) = \begin{cases} y_\mathrm{r} + c_\mathrm{a}\,\triangle T & \text{for } a_\mathrm{t} \vee a_\mathrm{n} \neq 0 \\ y_\mathrm{r} + \triangle t\, v_\mathrm{r}\cos\varphi_\mathrm{r} & \text{for } a_\mathrm{t} \wedge a_\mathrm{n} = 0 \end{cases}, \tag{27}
$$

$$
v(t) = v_\mathrm{r} + \triangle t\, a_\mathrm{t}\,, \tag{28}
$$

$$
\varphi(t) = \begin{cases} \varphi_\mathrm{r} + \frac{a_\mathrm{n}}{a_\mathrm{t}} \ln\left|1 + \triangle t \frac{a_\mathrm{t}}{v_\mathrm{r}}\right| & \text{for } a_\mathrm{t} \neq 0 \\ \varphi_\mathrm{r} + \triangle t\, \frac{a_\mathrm{n}}{v_\mathrm{r}} & \text{for } a_\mathrm{t} = 0 \end{cases}, \tag{29}
$$

where a_t and a_n are assumed constant.

A.2 Jacobian matrix of $\mathbf{f}[\mathbf{x}_\mathrm{r}; t, t_\mathrm{r}]$

Analogous to [8], the components of the Jacobian matrix of $\mathbf{f}[\mathbf{x}_\mathrm{r}; t, t_\mathrm{r}]$ are presented. The Jacobian matrix is given by

$$\left.\frac{\partial \mathbf{f}[\mathbf{x}_\mathrm{r}; t, t_\mathrm{r}]}{\partial \mathbf{x}_\mathrm{r}}\right|_{t=t_i} = \left.\begin{pmatrix} 1 & 0 & \frac{\partial x(t)}{\partial v_\mathrm{r}} & \frac{\partial x(t)}{\partial \varphi_\mathrm{r}} & \frac{\partial x(t)}{\partial a_\mathrm{t}} & \frac{\partial x(t)}{\partial a_\mathrm{n}} \\ 0 & 1 & \frac{\partial y(t)}{\partial v_\mathrm{r}} & \frac{\partial y(t)}{\partial \varphi_\mathrm{r}} & \frac{\partial y(t)}{\partial a_\mathrm{t}} & \frac{\partial y(t)}{\partial a_\mathrm{n}} \\ 0 & 0 & 1 & 0 & \triangle t & 0 \\ 0 & 0 & \frac{\partial \varphi(t)}{\partial v_\mathrm{r}} & 1 & \frac{\partial \varphi(t)}{\partial a_\mathrm{t}} & \frac{\partial \varphi(t)}{\partial a_\mathrm{n}} \\ 0 & 0 & 0 & 0 & 1 & 0 \\ 0 & 0 & 0 & 0 & 0 & 1 \end{pmatrix}\right|_{t=t_i} . \quad (30)$$

For the partial derivations of $\varphi(t)$ (29), we have

$$\frac{\partial \varphi(t)}{\partial v_\mathrm{r}} = -\frac{\triangle t\, a_\mathrm{n}}{v_\mathrm{r}(v_\mathrm{r} + \triangle t\, a_\mathrm{t})} ,$$

$$\frac{\partial \varphi(t)}{\partial a_\mathrm{t}} = \begin{cases} \frac{a_\mathrm{n}}{a_\mathrm{t}} \left(-\frac{\partial \varphi(t)}{\partial v_\mathrm{r}} + \frac{\triangle t}{v_\mathrm{r} + \triangle t\, a_\mathrm{t}} \right) & \text{for } a_\mathrm{t} \neq 0 \\ -\frac{\triangle t^2}{2} \frac{a_\mathrm{n}}{v_\mathrm{r}^2} & \text{for } a_\mathrm{t} = 0 \end{cases} ,$$

$$\frac{\partial \varphi(t)}{\partial a_\mathrm{n}} = \begin{cases} \frac{1}{a_\mathrm{t}} \ln \left| 1 + \triangle t \frac{a_\mathrm{t}}{v_\mathrm{r}} \right| & \text{for } a_\mathrm{t} \neq 0 \\ \triangle t \frac{1}{v_\mathrm{r}} & \text{for } a_\mathrm{t} = 0 \end{cases} .$$

The partial derivations of $x(t)$ (26) are given by

$$\frac{\partial x(t)}{\partial v_\mathrm{r}} = \begin{cases} c_\mathrm{a} \left(2\frac{S(t)}{v(t)} + \frac{\partial \varphi(t)}{\partial v_\mathrm{r}} T(t) - 2\frac{S(t_\mathrm{r})}{v_\mathrm{r}} \right) & \text{for } a_\mathrm{t} \vee a_\mathrm{n} \neq 0 \\ \triangle t\, \sin \varphi_\mathrm{r} & \text{for } a_\mathrm{t} \wedge a_\mathrm{n} = 0 \end{cases} ,$$

$$\frac{\partial x(t)}{\partial \varphi_\mathrm{r}} = \begin{cases} c_\mathrm{a}\, \triangle T & \text{for } a_\mathrm{t} \vee a_\mathrm{n} \neq 0 \\ \triangle t\, v_\mathrm{r} \cos \varphi_\mathrm{r} & \text{for } a_\mathrm{t} \wedge a_\mathrm{n} = 0 \end{cases} ,$$

$$\frac{\partial x(t)}{\partial a_\mathrm{t}} = \begin{cases} -8 a_\mathrm{t} c_\mathrm{a}^2\, \triangle S + c_\mathrm{a} P(t) & \text{for } a_\mathrm{t} \vee a_\mathrm{n} \neq 0 \\ \frac{\triangle t^2}{2} \sin \varphi_\mathrm{r} & \text{for } a_\mathrm{t} \wedge a_\mathrm{n} = 0 \end{cases} ,$$

$$\frac{\partial x(t)}{\partial a_\mathrm{n}} = \begin{cases} -2 a_\mathrm{n} c_\mathrm{a}^2\, \triangle S + c_\mathrm{a} Q(t) & \text{for } a_\mathrm{t} \vee a_\mathrm{n} \neq 0 \\ \frac{\triangle t^2}{2} \cos \varphi_\mathrm{r} & \text{for } a_\mathrm{t} \wedge a_\mathrm{n} = 0 \end{cases} ,$$

where

$$P(t) = \frac{2\triangle t}{v(t)} S(t) + \frac{\partial \varphi(t)}{\partial a_\mathrm{t}} T(t) + 2v^2(t) \sin \varphi(t) - 2v_\mathrm{r}^2 \sin \varphi_\mathrm{r} ,$$

$$Q(t) = \frac{\partial \varphi(t)}{\partial a_\mathrm{n}} T(t) - v^2(t) \cos \varphi(t) + v_\mathrm{r}^2 \cos \varphi_\mathrm{r} .$$

Finally, we obtain for the partial derivations of $y(t)$ (27)

$$\frac{\partial y(t)}{\partial v_\mathrm{r}} = \begin{cases} c_\mathrm{a} \left(2\frac{T(t)}{v(t)} + \frac{\partial \varphi(t)}{\partial v_\mathrm{r}} S(t) - 2\frac{T(t_\mathrm{r})}{v_\mathrm{r}} \right) & \text{for } a_\mathrm{t} \vee a_\mathrm{n} \neq 0 \\ \triangle t\, \cos \varphi_\mathrm{r} & \text{for } a_\mathrm{t} \wedge a_\mathrm{n} = 0 \end{cases} ,$$

$$\frac{\partial y(t)}{\partial \varphi_\mathrm{r}} = \begin{cases} -c_\mathrm{a}\, \triangle S & \text{for } a_\mathrm{t} \vee a_\mathrm{n} \neq 0 \\ -\triangle t\, v_\mathrm{r} \sin \varphi_\mathrm{r} & \text{for } a_\mathrm{t} \wedge a_\mathrm{n} = 0 \end{cases} ,$$

$$\frac{\partial y(t)}{\partial a_\mathrm{t}} = \begin{cases} -8 a_\mathrm{t} c_\mathrm{a}^2\, \triangle T + c_\mathrm{a} U(t) & \text{for } a_\mathrm{t} \vee a_\mathrm{n} \neq 0 \\ \frac{\triangle t^2}{2} \cos \varphi_\mathrm{r} & \text{for } a_\mathrm{t} \wedge a_\mathrm{n} = 0 \end{cases} ,$$

$$\frac{\partial y(t)}{\partial a_\mathrm{n}} = \begin{cases} -2 a_\mathrm{n} c_\mathrm{a}^2\, \triangle T + c_\mathrm{a} V(t) & \text{for } a_\mathrm{t} \vee a_\mathrm{n} \neq 0 \\ \frac{\triangle t^2}{2} \sin \varphi_\mathrm{r} & \text{for } a_\mathrm{t} \wedge a_\mathrm{n} = 0 \end{cases} .$$

with

$$U(t) = \frac{2\triangle t}{v(t)} T(t) + \frac{\partial \varphi(t)}{\partial a_\mathrm{t}} S(t) + 2v^2(t) \cos \varphi(t) - 2v_\mathrm{r}^2 \cos \varphi_\mathrm{r} ,$$

$$V(t) = \frac{\partial \varphi(t)}{\partial a_\mathrm{n}} S(t) - v^2(t) \sin \varphi(t) + v_\mathrm{r}^2 \sin \varphi_\mathrm{r} .$$

References

[1] K. Becker, "Target Motion Analysis (TMA)," in *Advanced Signal Processing Handbook*, S. Stergioulos, Ed. New York, NY: CRC Press, 2001, ch. 9, pp. 284–301.

[2] ——, "A general approach to TMA observability from angle and frequency measurements," *IEEE Trans. Aerosp. Electron. Syst.*, vol. 32, pp. 487–494, Jan. 1996.

[3] R. A. Best and J. P. Norton, "A new model and efficient tracker for a target with curvilinear motion," *IEEE Trans. Aerosp. Electron. Syst.*, vol. 33, pp. 1030–1037, Jul. 1997.

[4] B. Ristic and M. S. Arulampalam, "Tracking a manoeuvring target using angle-only measurements: algortihms and performance," *IEEE Trans. Signal Processing*, vol. 83, pp. 1223–1238, 2003.

[5] B. Ristic, M. S. Arulampalam, and N. Gordon, *Beyond the Kalman Filter: Particle Filters for Tracking Applications*. Boston, MA: Artech House, 2004.

[6] T. Kirubarajan, Y. Bar-Shalom, and D. Lerro, "Bearings-only tracking of maneuvering targets using a batch-recursive estimator," *IEEE Trans. Aerosp. Electron. Syst.*, vol. 37, pp. 770–780, Jul. 2001.

[7] J. P. Le Cadre and O. Tremois, "Bearings-only tracking for maneuvering sources," *IEEE Trans. Aerosp. Electron. Syst.*, vol. 34, pp. 179–193, Jan. 1998.

[8] K. Becker, "Passive Aufklärung manövrierender Ziele aus Winkel- und Frequenzmessungen," Research Establishment of Applied Science (FGAN), Wachtberg, FKIE Report 95, Apr. 2005, in German language.

[9] J. A. Nelder and R. Mead, "A simplex method for function minimization," *Computer Journal*, vol. 7, pp. 308–313, Jan. 1965.